ADVANCED OPTICAL MATERIALS
www.advopticalmat.de

Enhanced Cyan Photoluminescence and Stability of $CsPbBr_3$ Quantum Dots Via Surface Engineering for White Light-Emitting Diodes

Xingyi He, Tianfeng Li, Zifan Liang, Renming Liu, Xia Ran, Xiaojuan Wang, Lijun Guo,* and Caofeng Pan**

The emission of cyan light (470-500 nm) plays a vital role in the visible light spectrum and is essential for applications such as lighting, displays, and optical communication. Inorganic cesium lead bromide perovskite quantum dots ($CsPbBr_3$ PQDs) have made significant progress in the field of luminescence materials and devices, however, the lack of techniques to obtain highly emissive and stable cyan-emitting $CsPbBr_3$ PQDs has limited their device applications. Here, it is demonstrated that the complete surface passivation by treatment of didodecyldimethylammonium bromide (DDAB) and lead bromide, which can enhance the photoluminescence and stability of cyan emitting $CsPbBr_3$ PQDs. In particular, the photoluminescence quantum yield of $CsPbBr_3$ QDs can be greatly improved from 10.5% to 83.8%. Through an effective PMMA passivation, the obtained stable and bright $CsPbBr_3$ PQDs composite films as the cyan color converters can effectively emit the cyan light to fill the "cyan gap" of white light-emitting diode (WLED). The color rendering index value of such WLED is remarkably enhanced from 73.6 to 82.5. This study paves the way for the application of PQD color converters in the next generation of full-visible-spectrum WLED lighting.

1. Introduction

All-inorganic metal halide $CsPbX_3$ (X = Cl, Br, and I) perovskite quantum dots (PQDs) have attracted intensive studies, due to their unique optical properties, such as size-dependent emission wavelength, narrow emission spectrum, and high luminescent efficiency.[1–3] Significant advancements have been made in the green and red PQDs, substantial progress has been achieved in green, yellow, and red PQDs.[4,5] Despite the abundant research progress in the above-mentioned luminous regions, studies on cyan-emitting PQDs for white light-emitting diode (WLED) lighting technologies are still lacking. Integrating a blue-emitting InGaN LED chip with YAG: Ce^{3+} yellow-emitting phosphors was a relatively established method of achieving WLED. However, this method has several drawbacks because red-light components are not present, such as low color rendering index (CRI, Ra < 75), blue light hazard and the "cyan gap" in the 470–520 nm range.[6–14] In the meantime, "full-visible-spectrum lighting" has been proposed to obtain a high-CRI light source that can mimic natural sunlight.[15] There, the development of fluorescent materials emitting cyan light can fill in the blue-green cavity in the spectrum of traditional phosphor-converted LEDs with improved CRI value.[16] However, in common inorganic LEDs, the cyan emission is substantially weaker, component-missing, and/or of poor optical performance. Due to their ultra-high color purity and broad color range, PQDs may be more appropriate for developing cyan light emitters than conventional gallium nitride-based emitters. Considering the challenges mentioned above, the development of cyan-emissive PQDs with satisfying optical performance is highly in demand.

Perovskite photoluminescence intensity and stability are crucial for enhancing device performance in practical applications. Engineering the surface defects has shown to be a highly efficient method for enhancing the photoluminescence of $CsPbBr_3$ QDs.[17–23] For instance, Xie et al. reported the synthesis of $CsPbBr_3$:xNd^{3+} QDs by incorporating Nd^{3+} as dopants into $CsPbBr_3$ QDs. The emission peaks could be finely tuned at 484, 494, and 515 nm with photoluminescence quantum yield (PLQY) values ranging from 75 to 90% through Nd^{3+} doping.[24] Hu et al. demonstrated the preparation of DDAB-$CsPbCl_{0.8}Br_{2.2}$ PQDs, exhibiting intense cyan emission while achieving a remarkable enhancement in PLQY from 12.2% to 83.1%. This improvement

X. He, T. Li, Z. Liang, L. Guo
School of Physics and Electronics, International Joint Research Laboratory of New Energy Materials and Devices of Henan Province
Henan University
Kaifeng 475004, P. R. China
E-mail: litianfeng@henu.edu.cn; juneguo@henu.edu.cn
R. Liu, X. Ran, X. Wang, L. Guo
Academy for Advanced Interdisciplinary Studies, School of Physics and Electronics
Henan University
Kaifeng 475004, P. R. China
C. Pan
Institute of Atomic Manufacturing
Beihang University
Beijing 100191, P. R. China
E-mail: pancaofeng@buaa.edu.cn
The ORCID identification number(s) for the author(s) of this article can be found under https://doi.org/10.1002/adom.202302726

DOI: 10.1002/adom.202302726

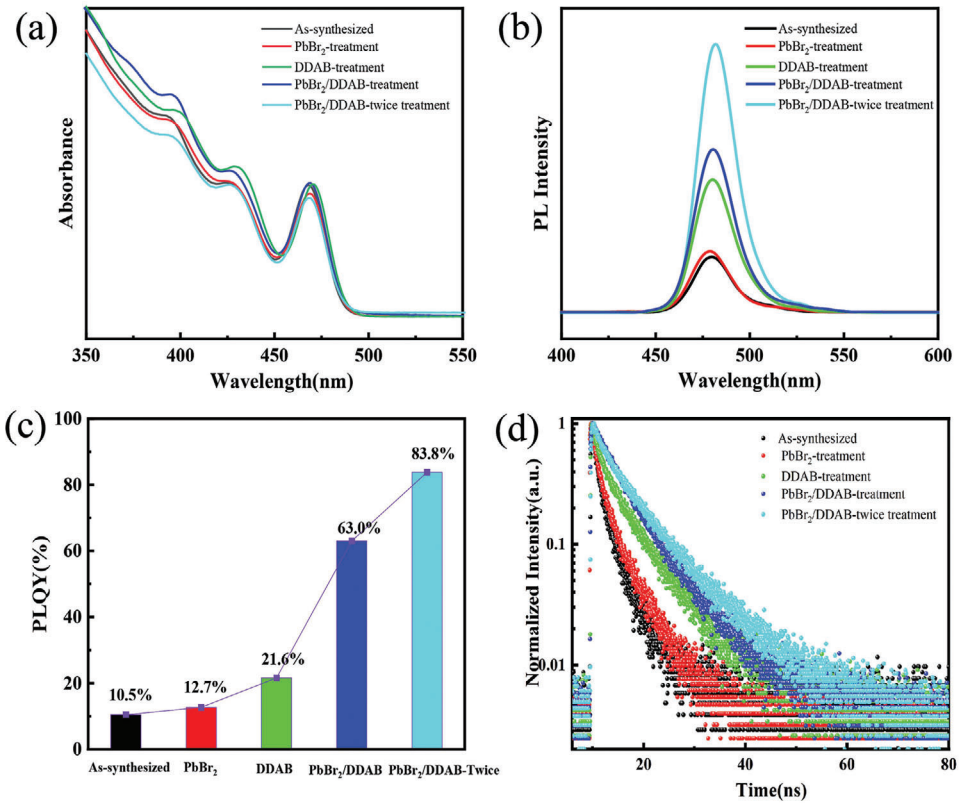

Figure 1. UV–vis absorption a) PL spectra b) PLQY c) and TRPL decay d) of as-synthesized, $PbBr_2$-treatment, DDAB-treatment, $PbBr_2$/DDAB treatment, and $PbBr_2$/DDAB-twice treatment C-PQDs.

was attributed to the reduction of surface defects through ligand exchange and halogen-compensation strategies.[25] Nevertheless, the migration of halogen ions often leads to undesirable perovskite phase segregation under prolonged radiation and joule heat. However, the progress in utilizing these cyan QDs as a solid-state component in WLED lighting devices is still limited. Furthermore, achieving working stability for practical applications remains a significant challenge.[26–28] The unstable ionic bond between the surface atoms of PQD and their oleic acid/oleylamine (OA/OAm) ligands results in easy stripping of the Pb atoms from the PQD surface, leading to unstable material storage and processing. This also reduces the PLQY of PQDs when exposed to continuous light irradiating for extended periods.[12,29,30] To enhance the stability of PQDs, numerous efforts have been made in recent years.[31] Chen's group discovered that substituting Pb with Mn (II) [32] in $CsPbBr_3$ could increase the formation energies of perovskite lattices and significantly improve the stability of PQDs. Surface ligand passivation is another commonly used technique,[33] where some groups treated the PQDs by introducing DDAB.[34–39] For example, Liu et al.[37] reported $CsPbBr_3$ QDs with a high solubility of 150 g L^{-1} in toluene and good film-forming properties. This was accomplished by anchoring a dense binary-ligand system, comprising branched and long-chain DDAB and octanoic acid, onto the surface of the QDs. In this process, DDAB replaces OA and OAm on the surface of PQDs, providing enhanced passivation. DDA^+ with two long hydrophobic chains ($2C_n$) is known to form more stable monolayers due to its favorable match with negatively charged surface sites' densities. However, studies focusing on achieving bright cyan emission from $CsPbBr_3$ QDs are relatively scarce.

In this work, we report that the combined treatment with DDAB and lead bromide can enhance the PLQY and stability of cyan-emitting $CsPbBr_3$ PQDs (C-PQDs), the PL peak position of the C-PQDs at ≈ 480 nm. This procedure results in robust colloids, which enhance the PLQY of the C-PQDs from 10.5% to 83.8%. Through an effective PMMA passivation, the stable and bright C-PQDs composite films as the cyan color converters are used to fill the "cyan gap" of a WLED. Such WLEDs exhibit excellent luminescent performance with a CRI of 82.5, much higher than the conventional WLEDs (73.6). The stable output of WLED enabled by sterical stabilization is useful to pave the way toward commercialization.

2. Results and Discussion

2.1. Photoluminescence Properties of C-PQDs

The C-PQDs were synthesized using a modified hot injection method (**Figure 1**),[40] the obtained C-PQDs were dispersed in toluene (step 1). To improve the photoluminescence and stability of C-PQDs, the comprehensive surface structure passivation process was implemented as presented in Scheme S1 (Supporting Information). Both DDAB and $PbBr_2$ ($PbBr_2$/DDAB-

treatment) stock solution was added to the as-synthesized C-PQDs solution and stirred for 2 h to exchange OA/OAm ligands (step 2), as a comparison, only $PbBr_2$ or DDAB stock solution was also added into C-PQDs for ligand exchange ($PbBr_2$-treatment or DDAB-treatment). Methyl acetate was used to further purify the $PbBr_2$/DDAB-treatment C-PQDs to get rid of extra DDAB and other by-products (step 3). Figure 1a illustrates the absorption spectra of C-PQDs with different surface treatments. The well-defined band-edge exciton transition peak at 470 nm is observed along with peaks at higher energies, specifically at ≈ 430 and 390 nm, indicating strong quantum confinement effects. Figure 1b shows the emission spectra at 480 nm of C-PQDs treated with different ligands. Compared to the as-synthesized C-PQDs, the PL intensity increased by ≈ 10% for $PbBr_2$-treatment C-PQDs, while it increased by about two-and-a-half times for DDAB-treatment $CsPbBr_3$ QDs and three times for $PbBr_2$/DDAB-treatment $CsPbBr_3$ QDs. The addition of both $PbBr_2$ and DDAB is based on theoretical considerations,[41] suggesting that it may help rebuild damaged $PbBr_6$ octahedra during purification procedures. Therefore, combining $PbBr_2$ with DDAB appears more effective than using $PbBr_2$ alone. It should be noted that while $PbBr_2$ alone is not soluble in toluene, it readily dissolves upon adding DDAB, forming an adduct, possibly $DDAPbBr_3$ and/or DDA_2PbBr_4. The addition of DDAB alone or preferably DDAB +$PbBr_2$ (in a 2:1 molar ratio) enhances the PL intensity of QDs. After purification, the PL intensity of the $PbBr_2$/DDAB-treatment C-PQDs slightly decreased. To compensate for the loss of an adduct during purification, we added an adduct to the solution (step 4) and found that it increased in PL intensity, the PLQY also increased from 10.5% for the as-synthesized C-PQDs to 12.7%, 21.6%, 63.0%, and 83.8% for $PbBr_2$-treatment, DDAB-treatment, $PbBr_2$/DDAB-treatment, and $PbBr_2$/DDAB-twice treatment C-PQDs respectively (Figure 1c). We added $PbBr_2$/DDAB once more (thrice treatment), and found the PL intensity and stability of C-PQDs decreased slightly (Figures S1 and S2, Supporting Information), We think $PbBr_2$/DDAB-twice treatment C-PQDs may have the highest ligand density, $PbBr_2$/DDAB-thrice treatment could not increase ligand density more. Additional treatment may weaken the PL intensity and stability of C-PQDs. It is important to note that PLQYs were measured relative to quinine sulfate by comparing integrated intensities while accounting for the absorbance at the excitation wavelengths (Supporting Information). C-PQDs treated with $PbBr_2$/DDAB can undergo multiple rounds of precipitation and redispersion without losing their properties; at least three such cycles were observed in our study. However, these rigorous purification procedures do not apply to the as-synthesized C-PQDs as they become insoluble after just one round of purification treatment. This observation further highlights the robustness provided by the coating with $PbBr_2$/DDAB. Figure 1d shows their corresponding time-resolved PL-fitted decay curves. The average lifetime (τ_{avg}, extracted from biexponential fits; see Table S1, Supporting Information) of as-synthesized, $PbBr_2$-treatment, DDAB-treatment, $PbBr_2$/DDAB-treatment, and $PbBr_2$/DDAB-twice treatment C-PQDs were 2.68, 3.42, 5.72, 6.89, and 7.44 ns, respectively. It could be easily seen that the τ_{avg} of the as-synthesized C-PQDs became the longest after the treatment with $PbBr_2$/DDAB-twice treatment. A similar reduction in decay rate was observed when $CsPbI_3$ QDs were passivated by triphenylphosphine.[42,43] A slower relaxation rate indicates a lower density of traps, which can be used as local sites for nonradiative recombination,[44] and is in line with the enhanced PLQY, indicating the successful passivation of surface defects.

2.2. Structural Characterization

Transmission electron microscope (TEM) and X-ray diffraction (XRD) analyses were conducted to access the detailed structure of these C-PQDs. Figures 2a,b and Figure S3 (Supporting Information) show the morphology and size histogram of $PbBr_2$/DDAB-twice treatment C-PQDs and as-synthesized, $PbBr_2$-treatment, DDAB-treatment, $PbBr_2$/DDAB-treatment C-PQDs. The size distribution of all samples is summarized and shows an average particle size of ac. 4.0 nm and undergo no obvious change before and after the treatment. As shown in Figure S3a (Supporting Information) and **Figure 2a**, $CsPbBr_3$ C-PQDs treated with and without $PbBr_2$/DDAB have the same crystal lattices with a lattice spacing of distance of 0.33 nm, which corresponds to the plane lattice spacing of (111). The drop-casting method was used to obtain C-PQDs on a mica sheet for the AFM measurements, in which the concentration of QDs was 0.005 mg mL^{-1}. In the presence of C-PQDs, some uniformly dispersed points can be seen in the mica sheet. The C-PQDs had a height of ≈ 4.2 nm, which is almost consistent with the observations in TEM images (Figure S4, Supporting Information). Figure S5 (Supporting Information) shows the XRD patterns of all samples of C-PQDs. While as-synthesized C-PQDs exhibit diffraction peaks at 15.23°, 21.55°, 30.43°, 34.42°, 37.86° and 43.82°, which correspond to (100), (110), (200), (210), (211) and (202) planes of $CsPbBr_3$ QDs (JCPDS 54–0752), respectively. Similar diffraction peaks are found for the other samples, indicating that these treatments have a negligible influence on the crystalline.

Fourier Transform Infrared spectra (FTIR) of as-synthesized, $PbBr_2$/DDAB-twice treatment (for simple, marked post-treated) C-PQDs were recorded to investigate the surface properties. As shown in Figure 2c, the vibration bands in the range of 2840–2950 cm^{-1} can be attributed to the C—H stretching vibration of CH_2 and CH_3, while the peaks at 1466 cm^{-1} are attributed to CH_2 bending vibration.[34] Compared with the as-synthesized C-PQDs, there is a significant decrease in the N—H stretching (3006 cm^{-1}) vibration mode of the amine group in the FTIR spectra of the post-treated C-PQDs.[45] Additionally, two absorption peaks at 1530, and 1404 cm^{-1} that can be assigned to C═O stretching vibrations of the carboxylate group, and asymmetric/symmetric vibrations of alkyl carbon chains from OA and OAm also show a dramatic decrease for post-treated C-PQDs. The characteristic peak for DDA^+ cation's C-N^+ appears at 1050 cm^{-1},[25,46] further confirming ligand exchange from OAm and OA to DDA^+.

The element compositions were determined by X-ray photoelectron spectroscopy (XPS) in order to demonstrate the impact of $PbBr_2$/DDAB on the surface state of samples. The XPS results in Figure 2d show N1s core level for both as-synthesized and post-treated C-PQDs. For the as-synthesized C-PQDs, peaks at 398.8 and 401.3 eV originate from the amine group (-NH_2) and protonated amine group (-NH^{3+}) present in OA and OAm

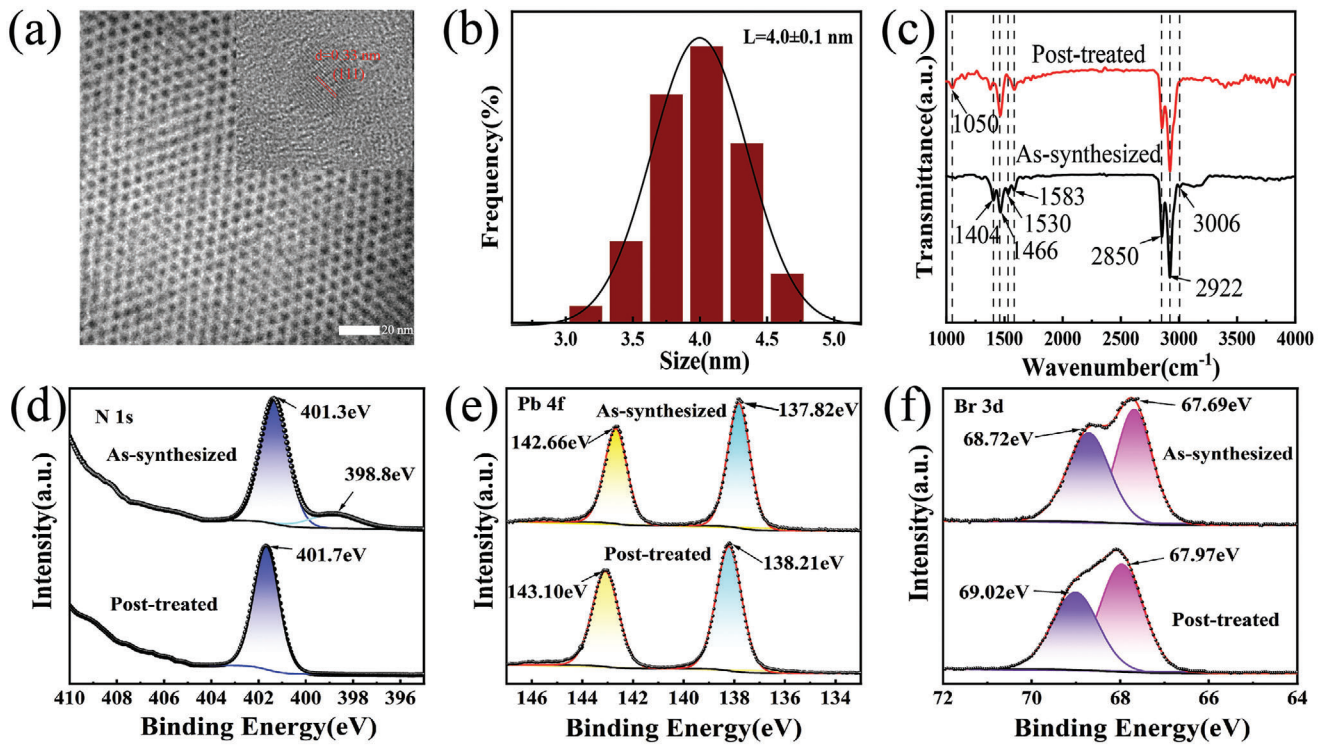

Figure 2. HRTEM a) and the size histogram b) of $PbBr_2$/DDAB-twice treatment C-PQDs; c) FTIR of as-synthesized and $PbBr_2$/DDAB-twice treated C-PQDs. High-resolution XPS spectra of d) N1s, e) Pb 4f, and f) Br 3d for as-synthesized and post-treated (PbBr2/DDAB-twice treatment) C-PQDs.

respectively. However, post-treated C-PQDs exhibit a single peak at 401.7 eV corresponding to tert-ammonium cations from DDA^+ cations,[34,47] indicating successful ligand exchange with DDAB. Figure 2e,f display Pb 4f and Br 3d core levels for both C-PQDs. In Pb 4f XPS core level spectra, a higher binding energy shift of 0.4 eV was observed for post-treated C-PQDs (Figure 2e). Based on the QD model proposed by De Roo et al.,[48,49] we hypothesize that Pb atoms in $CsPbBr_3$ QDs are in two distinct chemical environments, with higher binding energy assigned to Pb-Br and lower binding energy assigned to Pb-ligand. Consequently, the higher binding energy shift observed in the Pb 4f spectrum of post-treated C-PQDs indicates an increase in the population of Pb-Br species compared to as-synthesized C-PQDs. This increase is further supported by the Br 3d spectrum, where higher binding energy regions correspond to Pb-Br and lower binding energy regions correspond to Cs-Br. The XPS results (Figure S6, Supporting Information) reveal a change in the ratio of Pb/Br atoms from 1:2.9 for as-synthesized to 1:3.1 for post-treated C-PQDs, indicating an increased presence of Pb-Br species after treatment. DDA^+ has a stronger affinity with the negative sites (Br^-) and large steric hindrance due to its branched structure,[43] so the DDAB surface ligand can increase steric hindrance and Br^- content.

The addition of DDAB (acting as a ligand) and $PbBr_2$ (for repairing the Pb-Br layer), or their adduct, has been found effective in enhancing PLQY and long-term durability. For $PbBr_2$/DDAB-twice treatment PQDs, it is believed that there is a greater abundance of DDAB on the surface of PQDs, which helps maintain high density and provides protection against degradation. The branched structure of DDA^+ leads to larger steric hindrance, resulting in fewer positive ions being adsorbed onto the PQDs surface,[34] and creating a rich-Br^- surface that enhances stability.[50,51]

2.3. Stability of C-PQDs

The lack of stability of the PQDs is a major limiting factor for their wide-scale applications. To pursue whether the $PbBr_2$/DDAB modification improves the stability of the post-treated C-PQDs, we here study their chemical stability using as-synthesized C-PQDs as a control group. First, the long-term stability of the C-PQDs is evaluated by monitoring the PLQY of their stock solution stored in ambient conditions. As shown in **Figure** 3a–c, the PLQY of post-treated C-PQDs does not exhibit substantial variations over time (30 days), testifying to the robustness of the passivation offered by the ligands. In comparison, the PLQY of as-synthesized C-PQDs stored in toluene is drastically degraded, dropping to values as low as 25% of its initial value during the same time.[52] The post-treated C-PQDs also exhibit much-improved photo-stability (3d-f). We expose our C-PQDs dispersed in toluene to UV irradiation (365 nm, 4 W). A rapid fluorescence decrease is found in the as-synthesized C-PQDs after 30 min continuous illumination of UV light and retained only 65% of its initial intensity (Figure 3d,f), which was primarily due to ligands (OA or OAm) falling off the surface of PQDs and additional structural

defects caused by UV irradiation.[53] In contrast, the PL intensity of post-treated C-PQDs experienced a relatively slower decrease and remained at almost 96% of its initial PL intensity after

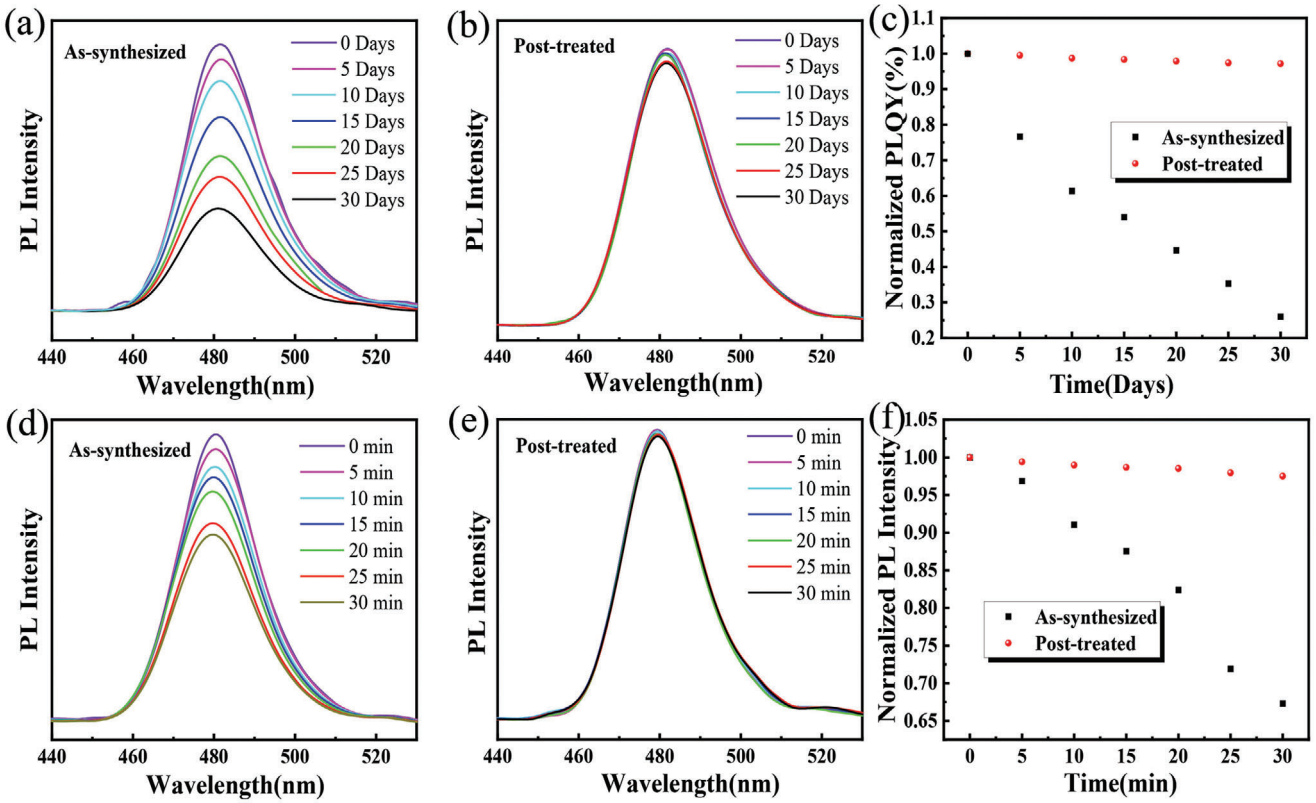

Figure 3. PL intensity of as-synthesized a) and post-treated b) C-PQDs over days, c) time-dependent normalized PLQY for these C-PQDs with different days; Under UV irradiation, PL intensity of as-synthesized d) and post-treated QDs e) over minutes, f) normalized PL intensity of these C-PQDs in UV light.

30 min continuous illumination of UV light, owing to the steric hindrance of DDA^+ on the surface of the PQDs.[43]

We examine the thermostability of C-PQDs at temperatures ranging from 273 to 333 K in the same ambient condition (**Figures** 4a–c). When the temperature is raised from 273 to 333 K, the PL intensity decreases rapidly for as-synthesized compared to post-treated C-PQDs. In contrast, the PL intensity of post-treated C-PQDs remains at 70% of its initial intensity at 333 K. This could be due to lower exciton binding energy and more defeat-associated exciton quenching.[54,55] Due to nonradiative recombination and deep-level defeat sites and energy states in the PQDs, low PLQY is mostly caused by these factors. The exciton binding energy is enhanced for post-treated compared to as-synthesized C-PQDs after defeat sites are effectively passivated under $PbBr_2$/DDAB treatment. Hence, there is not much change in the PL intensity for post-treated C-PQDs even up to 333 K due to suppressed nonradiative recombination sites with enhanced exciton binding energy.[54] As mentioned above, the post-treated C-PQDs solution shows far better stability than as-synthesized. Finally, we find that the post-treated C- PQDs exhibit significantly

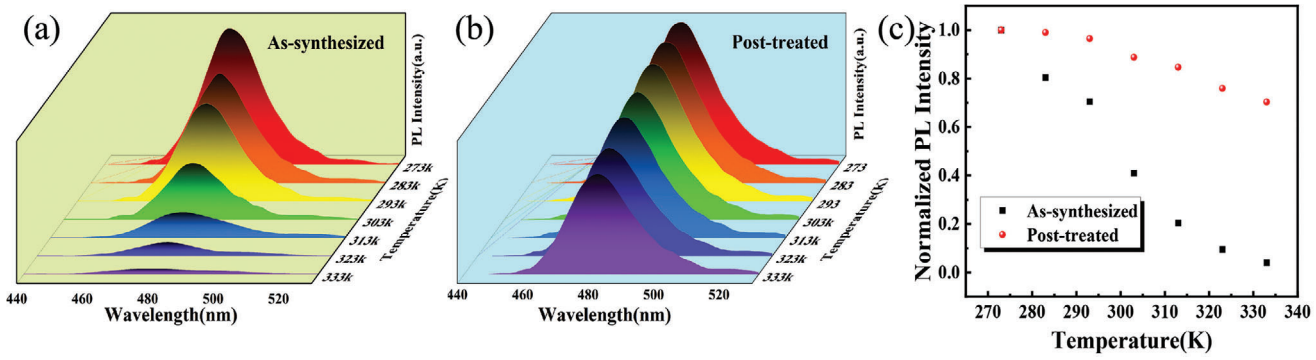

Figure 4. The change in PL peak intensity of as-synthesized a) and post-treated b) C-PQDs with different temperatures; c) The corresponding normalized PL Intensity as a function of temperature.

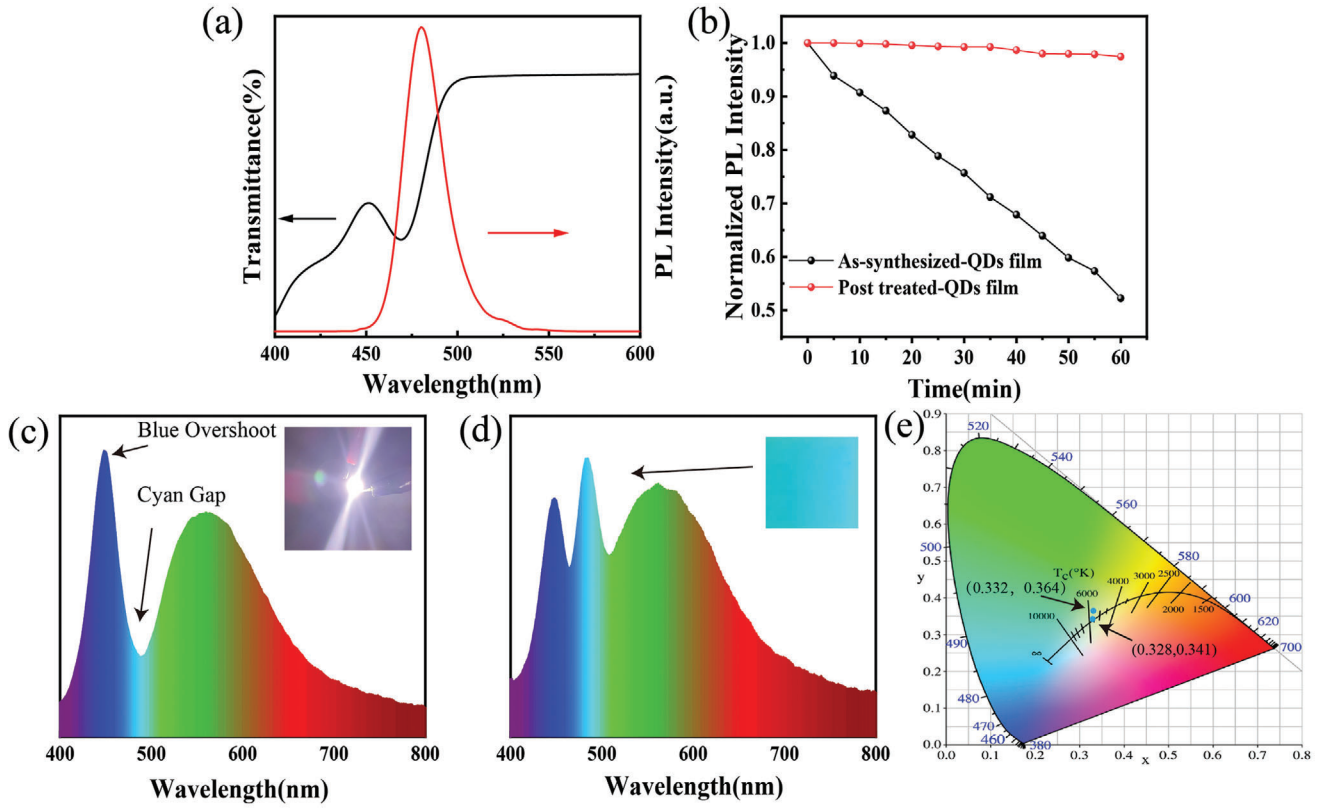

Figure 5. a) UV–vis transmittance spectrum and PL emission spectrum of the post-treated C-PQDs composite film. b) normalized PL intensity of C-PQD films under UV irradiation. Emission spectra of the 455 nm LED-excited lamps fabricated without c) and with d) C-PQDs composite films. The photograph of the lamp without cyan film in the inset of Figure 5c and the photograph of the 480 nm cyan emissive film under UV light in the inset of Figure 5d. e) CIE diagram of white LED with C-PQDs composite film.

improved stability compared to the as-synthesized C-PQDs under various conditions.

2.4. Application in WLEDs

In the practical application of the display, the fluorescent PQDs are used as down conversion phosphor incorporated into the polymer.[56] So, the C-PQD composite film could be obtained by encapsulating $CsPbBr_3$ in polymethyl methacrylate (PMMA). The thin films in this preparation were prepared using spin-coating procedures. First, PMMA was coated on the quartz substrate. And then, the post-treated C-PQDs solution was obtained by adding post-treated C-PQDs into the toluene solution, the C-PQDs solution was coated using spin coating on the PMMA film, further, the other PMMA was coated again. Thus, a uniform optical composite film was obtained. The UV–vis transmittance and PL emission spectra of the as-fabricated film are shown in **Figure** 5a, the emission peak of the film was at 480 nm. The film showed bright cyan emission when exposed to 365 UV light (Inset of Figure 5d). The films deposited by spin-coating of the QDs show uniform and crack-free morphology, and a smooth surface with a root-mean-square surface roughness of 6.1 nm (Figure S7, Supporting Information).

To evaluate the stability of the post-treated C-PQD composite film, we utilized the as-synthesized C-PQD composite film as a control group in subsequent experiments. Under intense UV light (365 nm, 18 W), Figure 5b and Figure S8 (Supporting Information) demonstrate that the PL intensity of the as-synthesized C-PQDs composite film decreased by 50% after 60 min of illumination. In contrast, the PL intensity of the post-treated C-PQD composite film only declined by 5% within the same time frame. This demonstrates that employing $PbBr_2$/DDBA ligands instead of OA/OAm is a more efficient approach to enhancing photostability in cyan-emitting PQD composite films. The degradation under UV light can be attributed to facile dissociation between as-synthesized C-PQDs and OA/OAm ligands due to their highly dynamic binding on the surface.[53] Continuous exposure promotes aggregation and growth into larger crystals with diminished fluorescence performance. However, DDAB's ion characteristics and two long carbon chains make it better at preventing excessive growth of C-PQDs.

To assess a potential application for $PbBr_2$/DDAB-treatment C-PQDs cyan converters in white LED lighting systems excited by 455 nm LED, we employed an as-fabricated C-PQD composite film as the cyan converters for white LED lamps. As depicted in Figure 5c,d, two identical commercial WLED lamps were selected to compare emission spectra between an LED without and an LED with a C-PQD composite film attached; photographs of these white commercial LEDs are shown in the inset image of Figure 5c. It can be observed that WLED lamps without a cyan film exhibit a deep blue-green cavity ranging from 450 and

550 nm along with excessive blue light emissions, resulting in Ra values of ≈ 73.6, and chromaticity coordinates of (0.328, 0.341). Conversely, when using an LED with a cyan film (Figure 5d), there is virtually no blue overshoot and the cyan gap is filled; this indicates that the as-fabricated C-PQD composite film as the cyan converters not only effectively absorb the extra blue light, and make up for the cyan "gap" of white LED lamps. More, a Ra of 82.5 is on the LED with cyan composite film, and the chromaticity coordinates (Figure 5e) are (0.332, 0.364), where saturated blue R12 rises from 49 to 80, demonstrating the application potential of the device in full-spectrum illumination for improved color rendition.

3. Conclusion

In summary, highly efficient C-PQDs for healing the surface trap states and for improving the stability by the combined treatment with DDAB and lead bromide are successfully developed, and the fluorescence emission of C-PQDs with 480 nm. The post-treated C-PQDs show outstanding cyan emission with a high PLQY of 83.8% and substantially enhanced photo- and thermal stability. The $PbBr_2$/DDAB post-treated composite film was applied in the commercial WLED devices, as a result, the 455 nm blue LED exhibited well-distributed white light with an improved CRI of 82.5. This suggests that these cyan-emitting PQDs can be used for reducing blue overshoot and compensating for the blue-green cavity. All these characteristics and results position the obtained luminescent materials as promising candidates for high-color-quality lighting applications.

4. Experimental Section

Materials: Cesium Carbonate (Cs_2CO_3, 99.99%), and Lead (II) bromide ($PbBr_2$, 99.99%) were purchased from Xi'an Polymer Light Technology Corp. Oleylamine (OAm, 80–90%), Zinc bromide ($ZnBr_2$, 98%), toluene (anhydrous, 99.5%), methyl acetate (anhydrous, 99%), and 1-octadecene (ODE, 90%) were purchased from Aladdin reagent. Oleic acid (OA, 90%) and polymethylmethacrylate (PMMA, 99%) were purchased from Alfa Aesar reagent, and didodecyldimethylammonium bromide (DDAB, 99.8%) was purchased from Aldrich reagent.

Synthesis of C-PQDs: C-PQDs were synthesized by using a hot injection approach[40] with modifications. In order to synthesize the Cs-precursor solution, a 50 mL three-necked flask was used. 300 mg Cs_2CO_3, 1.2 mL OA, and 3.2 mL ODE were added, and the mixture was vacuum-dried at 120°C for one hour before being heated to 150 °C under an N_2 atmosphere for 10 min. Precursors of Cs-OA should be heated to temperatures over 100 °C before usage to prevent precipitation. Another 250 mL three-neck flask was used for mixing 700 mg $PbBr_2$, 1700 mg $ZnBr_2$, 14 mL OA, 14 mL OAm, and 40 mL ODE. The mixture was vacuum-dried for 1 h at 120°C and subsequently transferred to an N_2 atmosphere for 15 min. 3 mL of Cs precursor should be injected quickly. After 90 s of reaction, the solution was cooled with ice water. Removed the unreacted precursors from the solution by centrifuging it at 8000 rpm. Collected the supernatant, and then left the supernatant on a benchtop for 24 h until a white pellet emerged. After removing all remaining solids, combine the supernatant with 1:3 methyl acetate before centrifuging the mixture at 8000 rpm for 10 min to separate the pellet and dissolve it in toluene.

Surface Ligand Exchange with OA/OAm: 0.1 mmol of $PbBr_2$ and 0.2 mmol of DDAB were dissolved in 3 ml of toluene to prepare $PbBr_2$/DDAB stock solution, this solution was stirred for 2 h, lightly heated to 40–50°C to obtain a transparent solution. Added 100 µL of $PbBr_2$/DDAB stock solution to 800 µL of purified QDs solution and stirred for one hour. Added 2.7 mL of methyl acetate to the solution, and centrifuged at 8000 rpm for 5 min, The precipitation was dispersed in 500 µL toluene. Subsequently, 50 µL of $PbBr_2$/DDAB solution was again added to the QDs solution and stirred for one hour, dispersed into 500 µL toluene after the same purification step. In the control group experiments, the moles of $PbBr_2$ and DDAB were prepared and exchanged as the same as above.

Frication of C-PQDs Composite Films: The quartz substrate was cleaned sequentially in ultrasonic baths with detergent, deionized water, and ethanol. 25 mg mL^{-1} of the C-PQDs was dissolved in toluene. Subsequently, a toluene solution containing PMMA (50 mg mL^{-1}) was stirred at 80 °C until the powder was completely dissolved. The C-PQDs composite films were prepared using the spin coating method. First, 50 µL of PMMA/toluene solution was dropped to a clean quartz substrate and spun for 45 s at 4000 rpm. Next, 50 µL of C-PQDs /toluene was dropped and spun for 30 s at 4000 rpm. The film was then dried under vacuum for 30 min before another round of preparation to construct to complete the PMMA/C-PQDs/PMMA film preparation.

WLED Device Fabrication: The C-PQDs composite film was placed on the top of the light diffusing plate for WLED measurements.

Characterization: The absorption spectra of the C-PQDs solution were recorded using a PerkinElmer Lambda 35 spectrometer equipped with a quartz cell. The PL spectra were recorded at room temperature using a PerkinElmer LS55 fluorescence spectrometer. Fourier transform infrared (FTIR) spectra were obtained using a PerkinElmer spectrometer (Spectrum One B), where the C-PQDs samples were compressed into tablets. XRD (DX-2700) with monochromatic Cu Kα irradiation (λ = 1.54145A) was employed to analyze the crystalline phase of the C-PQDs samples in powder form within a test range of 10–90° for 2θ. TEM images were captured using a JEM-2100 microscope operating at an acceleration voltage of 200 kV. Samples for TEM measurement were prepared by drop-casting the dispersion of C-PQDs onto carbon-coated copper grids and evaporating the solvent at ambient temperature. For Time-Correlated Single-Photon Counting (TCSPC) measurements, the samples were excited by pulses from a broadband tunable femtosecond Ti: sapphire pulse laser source (Chameleon Ultra II, Coherent Inc.) generated via second harmonic generation from a BBO nonlinear crystal with a wavelength of 380 nm. The repetition rate of the excitation pulse was controlled by setting the Pockels cell (Conoptics, Model 305) to operate at a frequency of 40 MHz. X-ray photoelectron spectroscopy (XPS) analysis was conducted on a PHI 5000 Versa Probe delay line detector spectrometer equipped with an Al Kα monochromated X-ray source. The optical parameters of the fabricated WLEDs were measured using a PR670 spectrograph combined with an analyzer system.

Supporting Information

Supporting Information is available from the Wiley Online Library or from the author.

Acknowledgements

This work was supported by the National Natural Science Foundation of China (61805070, 22105063, 52125205, 52250398, U20A20166, 52192614 and 52003101), the Science and Technology Development Project of Henan Province (232102231036) and the Key Scientific Research Project of Colleges and Universities in Henan Province (Project no. 23A510013) and the National key R&D program of China (2021YFB3200302 and 2021YFB3200304).

Conflict of Interest

The authors declare no conflict of interest.

Data Availability Statement

The data that support the findings of this study are available from the corresponding author upon reasonable request.

Keywords

$CsPbBr_3$ QDs, cyan emitting, DDAB, photoluminescence quantum yield, white light-emitting diode

Received: October 26, 2023
Revised: December 14, 2023
Published online:

[1] L. Protesescu, S. Yakunin, M. I. Bodnarchuk, F. Krieg, R. Caputo, C. H. Hendon, R. X. Yang, A. Walsh, M. V. Kovalenko, *Nano Lett.* **2015**, *15*, 3692.
[2] S. B. Sun, D. Yuan, Y. Xu, A. F. Wang, Z. T. Deng, *ACS Nano* **2016**, *10*, 3648.
[3] Y. Z. Jiang, C. J. Sun, J. Xu, S. S. Li, M. H. Cui, X. L. Fu, Y. Liu, Y. Q. Liu, H. Y. Wan, K. Y. Wei, T. Zhou, W. Zhang, Y. G. Yang, J. Yang, C. C. Qin, S. Y. Gao, J. Pan, Y. F. Liu, S. Hoogland, E. H. Sargent, J. Chen, M. J. Yuan, *Nature* **2022**, *612*, 679.
[4] Y. Z. Wang, C. D. Xie, X. C. Yao, Q. L. Chen, W. N. Liu, Y. J. Fu, Q. M. Liu, J. S. Li, Y. L. Li, D. Y. He, *J. Materiomics* **2022**, *8*, 358.
[5] M. Jiang, X. Zhang, F. Wang, *Nano Res. Energy* **2023**, *2*, e9120069.
[6] P. Chitapanya, C. Phuangsuwan, M. Ikeda, *Color Res. Appl.* **2022**, *47*, 1345.
[7] J. Mao, H. Lin, F. Ye, M. C. Qin, J. M. Burkhartsmeyer, H. Zhang, X. H. Lu, K. S. Wong, W. C. H. Choy, *ACS Nano* **2018**, *12*, 10486.
[8] M. Peng, S. B. Sun, B. Xu, Z. T. Deng, *Adv. Funct. Mater.* **2023**, *33*, 2300583.
[9] F. Bertolotti, G. Nedelcu, A. Vivani, A. Cervellino, N. Masciocchi, A. Guagliardi, M. V. Kovalenko, *ACS Nano* **2019**, *13*, 14294.
[10] J. Liang, B. Devakumar, L. L. Sun, S. Y. Wang, Q. Sun, X. Y. Huang, *J. Mater. Chem. C* **2020**, *8*, 4934.
[11] F. Locardi, M. Samoli, A. Martinelli, O. Erdem, D. V. Magalhaes, S. Bals, Z. Hens, *ACS Nano* **2021**, *15*, 17729.
[12] Y. Y. Shen, H. L. Tang, F. Liu, K. B. Lin, J. X. Lu, C. A. Z. Yan, W. J. Feng, K. K. Liu, L. Q. Wu, M. J. Li, Z. H. Wei, K. Y. Yan, *Chem. Eng. J.* **2021**, *423*, 130160.
[13] M. Karlsson, Z. Y. Yi, S. Reichert, X. Y. Luo, W. H. Lin, Z. Y. Zhang, C. X. Bao, R. Zhang, S. Bai, G. H. J. Zheng, P. P. Teng, L. Duan, Y. Lu, K. B. Zheng, T. Pullerits, C. Deibel, W. D. Xu, R. Friend, F. Gao, *Nat. Commun.* **2021**, *12*, 361.
[14] D. X. Ma, P. Todorovic, S. Meshkat, M. I. Saidaminov, Y. K. Wang, B. Chen, P. C. Li, B. Scheffel, R. Quintero-Bermudez, J. Z. Fan, Y. T. Dong, B. Sun, C. Xu, C. Zhou, Y. Hou, X. Y. Li, Y. T. Kang, O. Voznyy, Z. H. Lu, D. Y. Ban, E. H. Sargent, *J. Am. Chem. Soc.* **2020**, *142*, 5126.
[15] X. Y. Huang, *Sci. Bull.* **2019**, *64*, 1649.
[16] Y. F. Liu, J. Silver, R. J. Xie, J. H. Zhang, H. W. Xu, H. Z. Shao, J. Jiang, H. C. Jiang, *J. Mater. Chem. C* **2017**, *5*, 12365.
[17] M. Y. Liu, L. Ma, K. H. Xie, P. P. Zeng, S. J. Wei, F. Zhang, C. Li, F. J. Wang, *J. Phys. Chem. Lett.* **2022**, *13*, 1519.
[18] A. Krishna, M. A. A. Kazemi, M. Sliwa, G. N. M. Reddy, L. Delevoye, O. Lafon, A. Felten, M. T. Do, S. Gottis, F. Sauvage, *Adv. Funct. Mater.* **2020**, *30*, 1909737.
[19] W. Li, J. Zhan, X. R. Liu, J. F. Tang, W. J. Yin, O. V. Prezhdo, *Chem. Mater.* **2021**, *33*, 1285.
[20] D. P. Nenon, K. Pressler, J. Kang, B. A. Koscher, J. H. Olshansky, W. T. Osowiecki, M. A. Koc, L. W. Wang, A. P. Alivisatos, *J. Am. Chem. Soc.* **2018**, *140*, 17760.
[21] Q. X. Zhong, M. H. Cao, Y. F. Xu, P. L. Li, Y. Zhang, H. C. Hu, D. Yang, Y. Xu, L. Wang, Y. Y. Li, X. H. Zhang, Q. Zhang, *Nano Lett.* **2019**, *19*, 4151.
[22] D. Yoo, J. Y. Woo, Y. Kim, S. W. Kim, S. H. Wei, S. Jeong, Y. H. Kim, *J. Phys. Chem. Lett.* **2020**, *11*, 652.
[23] X. B. Li, W. T. Huang, R. R. Zhang, Y. Guo, H. J. Yang, X. Y. He, M. X. Yu, L. X. Wang, Q. T. Zhang, *Rare Met.* **2022**, *41*, 1230.
[24] Y. X. Xie, J. N. Jiang, Q. Y. Tang, H. B. Zou, X. Zhao, H. M. Liu, D. Ma, C. L. Cai, Y. Zhou, X. J. Chen, J. Pu, P. F. Liu, *Adv. Sci.* **2020**, *7*, 1903323.
[25] X. B. Hu, Y. Q. Xu, J. C. Wang, J. X. Ma, L. J. Wang, W. Jiang, *Laser Photonics Rev.* **2023**, *17*, 2200280.
[26] J. Y. Tong, J. J. Wu, W. Shen, Y. K. Zhang, Y. Liu, T. Zhang, S. M. Nie, Z. T. Deng, *ACS Appl. Mater. Interfaces* **2019**, *11*, 9317.
[27] F. Gao, J. H. Wu, Y. L. Zhao, T. L. Song, Z. T. Deng, P. Wang, Y. G. Wang, H. B. Li, *Nanoscale* **2021**, *13*, 10329.
[28] C. Jia, H. Li, X. W. Meng, H. B. Li, *Chem. Commun.* **2018**, *54*, 6300.
[29] C. Sun, Y. Zhang, C. Ruan, C. Y. Yin, X. Y. Wang, Y. D. Wang, W. W. Yu, *Adv. Mater.* **2016**, *28*, 10088.
[30] T. T. Xuan, J. J. Huang, H. Liu, S. Q. Lou, L. Y. Cao, W. J. Gan, R. S. Liu, J. Wang, *Chem. Mater.* **2019**, *31*, 1042.
[31] C. L. He, Z. Q. Meng, S. X. Ren, J. Li, Y. Wang, H. Wu, H. Bu, Y. Zhang, W. Z. Hao, S. L. Chen, R. R. Yan, H. Liu, Y. F. Zhu, J. J. Zhao, *Rare Met.* **2023**, *42*, 1624.
[32] S. H. Zou, Y. S. Liu, J. H. Li, C. P. Liu, R. Feng, F. L. Jiang, Y. X. Li, J. Z. Song, H. B. Zeng, M. C. Hong, X. Y. Chen, *J. Am. Chem. Soc.* **2017**, *139*, 11443.
[33] B. Y. Xu, S. Yang, X. W. Feng, T. J. Zhang, Z. H. Gao, Y. S. Zhao, *J. Materiomics* **2023**, *9*, 423.
[34] J. Pan, L. N. Quan, Y. B. Zhao, W. Peng, B. Murali, S. P. Sarmah, M. J. Yuan, L. Sinatra, N. M. Alyami, J. K. Liu, E. Yassitepe, Z. Y. Yang, O. Voznyy, R. Comin, M. N. Hedhili, O. F. Mohammed, Z. H. Lu, D. H. Kim, E. H. Sargent, O. M. Bakr, *Adv. Mater.* **2016**, *28*, 8718.
[35] Z. C. Li, L. Kong, S. Q. Huang, L. Li, *Angew. Chem., Int. Ed.* **2017**, *56*, 8134.
[36] W. L. Zheng, Z. C. Li, C. Y. Zhang, B. Wang, Q. G. Zhang, Q. Wan, L. Kong, L. Li, *Nano Res.* **2019**, *12*, 1461.
[37] Y. F. Liu, S. Tang, Z. J. Gao, X. W. Shao, X. L. Zhu, J. R. Ribé, T. Wågberg, L. Edman, J. Wang, *Nano Res.* **2023**, *16*, 10626.
[38] X. L. Zhu, Z. C. Pan, T. Y. Xu, X. W. Shao, Z. J. Gao, Q. Y. Xie, Y. P. Ying, W. Pei, H. Lin, J. Wang, X. S. Tang, W. W. Chen, Y. F. Liu, *Inorg. Chem.* **2023**, *62*, 9190.
[39] Y. F. Liu, S. Tang, J. P. Fan, E. Gracia-Espino, J. P. Yang, X. J. Liu, S. Kera, M. Fahlman, C. Larsen, T. Wågberg, L. Edman, J. Wang, *ACS Appl. Nano Mater.* **2021**, *4*, 1162.
[40] Y. T. Dong, T. Qiao, D. Kim, D. Parobek, D. Rossi, D. H. Son, *Nano Lett.* **2018**, *18*, 3716.
[41] M. I. Bodnarchuk, S. C. Boehme, S. ten Brinck, C. Bernasconi, Y. Shynkarenko, F. Krieg, R. Widmer, B. Aeschlimann, D. Gunther, M. V. Kovalenko, I. Infante, *ACS Energy Lett.* **2019**, *4*, 63.
[42] F. Liu, Y. H. Zhang, C. Ding, S. Kobayashi, T. Izuishi, N. Nakazawa, T. Toyoda, T. Ohta, S. Hayase, T. Minemoto, K. Yoshino, S. Y. Dai, Q. Shen, *ACS Nano* **2017**, *11*, 10373.
[43] C. Zheng, C. H. Bi, F. Huang, D. Binks, J. J. Tian, *ACS Appl. Mater. Interfaces* **2019**, *11*, 25410.
[44] J. Z. Song, T. Fang, J. H. Li, L. M. Xu, F. J. Zhang, B. N. Han, Q. S. Shan, H. B. Zeng, *Adv. Mater.* **2018**, *30*, 1805409.
[45] C. Y. Zhang, Q. Wan, B. Wang, W. L. Zheng, M. M. Liu, Q. G. Zhang, L. Kong, L. Li, *J. Phys. Chem. C* **2019**, *123*, 26161.
[46] X. W. Li, W. S. Cai, H. L. Guan, S. Y. Zhao, S. L. Cao, C. Chen, M. Liu, Z. G. Zang, *Chem. Eng. J.* **2021**, *419*, 129551.
[47] L. Zhu, C. X. Wu, S. Riaz, J. Dai, *J. Lumin.* **2021**, *233*, 117884.
[48] J. De Roo, M. Ibanez, P. Geiregat, G. Nedelcu, W. Walravens, J. Maes, J. C. Martins, I. Van Driessche, M. V. Koyalenko, Z. Hens, *ACS Nano* **2016**, *10*, 2071.
[49] J. Y. Woo, Y. Kim, J. Bae, T. G. Kim, J. W. Kim, D. C. Lee, S. Jeong, *Chem. Mater.* **2017**, *29*, 7088.
[50] A. Z. Pan, J. L. Wang, M. J. Jurow, M. J. Jia, Y. Liu, Y. S. Wu, Y. F. Zhang, L. He, Y. Liu, *Chem. Mater.* **2018**, *30*, 2771.

[51] X. M. Li, Y. Wu, S. L. Zhang, B. Cai, Y. Gu, J. Z. Song, H. B. Zeng, *Adv. Funct. Mater.* **2016**, *26*, 2435.
[52] R. Grisorio, F. Fasulo, A. B. Munoz-Garcia, M. Pavone, D. Conelli, E. Fanizza, M. Striccoli, I. Allegretta, R. Terzano, N. Margiotta, P. Vivo, G. P. Suranna, *Nano Lett.* **2022**, *22*, 4437.
[53] R. K. Gautam, S. Das, A. Samanta, *ChemNanoMat* **2022**, *8*, 202200029.
[54] M. R. Subramaniam, A. K. Pramod, S. A. Hevia, S. K. Batabyal, *J. Phys. Chem. C* **2022**, *126*, 1462.
[55] H. C. Woo, J. W. Choi, J. Shin, S. H. Chin, M. H. Ann, C. L. Lee, *J. Phys. Chem. Lett.* **2018**, *9*, 4066.
[56] J. L. Sun, T. S. Li, L. Dong, Q. L. Hua, S. Chang, H. Z. Zhong, L. J. Zhang, C. X. Shan, C. F. Pan, *Sci. Bull.* **2022**, *67*, 1755.